Evaporation of Metallic Exciton Droplets in Optically Pumped Germanium

J. C. Hensel, T. G. Phillips, and T. M. Rice
Bell Laboratories, Murray Hill, New Jersey 07974
(Received 22 November 1972)

High densities of excitons are produced in germanium at liquid-helium temperatures by a pulsed-laser pumping technique. The excitons condense into metallic droplets whose time decay, monitored by a cyclotron resonance method, is nonexponential and displays a cutoff. This is due to surface evaporation, and a measurement of the work function gives a value for the binding energy of the metallic liquid of $16(^{+3}_{-2})$ K which agrees with the value we find from observation of the threshold for the liquid phase.

In germanium at liquid-helium temperatures, high concentrations of indirect excitons can be readily generated by optical excitation. Experiments[1-4] suggest that a condensation occurs. There is also evidence that the condensed phase is metallic[3,5,6] and in the form of droplets[3,5-8] (sometimes called e-h droplets).

In this Letter we describe pulsed-laser pumping experiments in which cyclotron resonance is used to monitor free carriers. At a given temperature there is a threshold in pumping power above which a long-lived signal appears.[5] We interpret this to signify the presence of droplets of the liquid phase. From the strikingly nonexponential nature of the decay process we deduce that both internal decay and surface evaporation processes are active; and, in fact, we can observe a cutoff in the decay process where the droplets decay to zero volume. An analysis in terms of the rate equations allows us to measure the work function Φ which is equivalent to the metallic binding energy. A second value of Φ can be deduced from our measurements of the temperature dependence of the threshold power. The two values are in good agreement but are lower than some Φ's determined from luminescence experiments.[3,4]

The cyclotron-resonance experiments were performed using a sensitive superheterodyne microwave spectrometer operating at 53 GHz. The sample (dimensions $2.5\times2.5\times0.6$ mm^3) of high-purity Ge ($N_A - N_D \approx 1\times10^{10}$ cm^{-3}) was mounted strain free in the spectrometer cavity and immersed in the liquid-helium bath. Optical excitation at 1.064 μm was supplied by a neodymium-doped yttrium-aluminum-garnet Q-switched laser with a pulse width of 200 nsec. Temperature measurements with a superconducting bolometer (time constant $\sim10^{-7}$ sec) show that the temperature rise in the sample is not significant in the experiments reported here.

A typical decay curve is shown in the inset of Fig. 1, in which the amplitude of the signal measures the number of free electrons in the sample *outside* the regions of condensation. Cyclotron resonance inside the droplets is not seen, as the plasma frequency of the condensed phase[6] is

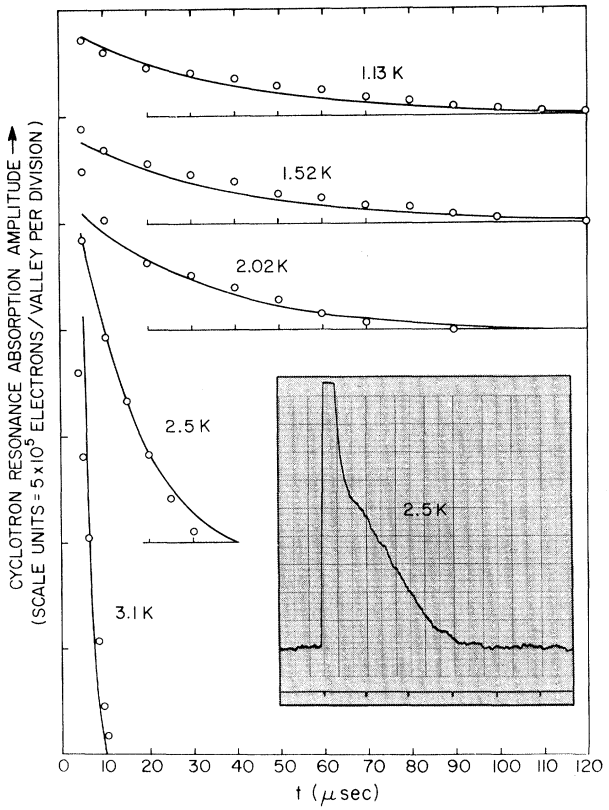

FIG. 1. Decay profiles of the electron cyclotron resonance signal subsequent to Q-switched laser excitation. The inset shows a typical tracing in which a fast signal coincident with the laser pulse is followed by a much slower, nonexponential decay terminated by an abrupt cutoff. In the main figure the solid curves are calculated from the rate equations; the circles represent the data. The data were recorded at a peak optical power level of 4×10^{-3} W (power density, 0.16 W/mm^2).

much higher than our operating frequency. The sequence of tracings in Fig. 1 shows that the decays are quasiexponential at low temperatures, but change markedly as the temperature increases, with a sharp cutoff developing for $T > 1.8$ K.

At low pumping powers there is no long-lived tail after the pulse, since the density created during the period of the light pulse (and in a volume determined by the exciton diffusion rate) is not great enough to cause condensation. If we fix the temperature and steadily increase the optical pumping power, we find a critical onset for the long-lived tail which signals the presence of the condensed phase.[5] A simple interpretation would suggest that this effect maps out part of the phase diagram (the coexistence curve) in temperature-density space as shown by the data in Fig. 2.

A further increase in pumping power increases the amount of condensed phase in the form of drops, until at a density of $n_0 \approx 2\times10^{17}$ cm^{-3} the whole medium would become metallic. The present experiments are well below this limit and are concerned with the creation and decay of the metallic drops in the two-phase region.

The behavior of the two-phase system after the light is switched off is described by a set of coupled rate equations.[3] We assume that the creation process gives a fixed number of droplets each containing ν electrons and ν holes, whose temperature is essentially that of the lattice. (The thermal relaxation time of the e-h liquid is short relative to a typical measurement time of ~ 1 μsec.)

The "volume" decay rate of the drop $(1/\tau_0)$ is the sum of the rates due to direct e-h recombination (luminescence) and Auger recombination with ejection of carriers from the drop $(1/\tau_A)$. Also, surface evaporation of e-h pairs as excitons will occur at a rate which depends exponentially (as in thermionic emission) on $\Phi/k_B T$. The number of e-h pairs in the drop is then given by

$$\dot{\nu} = -\nu/\tau_0 - aT^2\nu^{2/3}\exp(-\Phi/k_B T) + b\nu^{2/3}n_{ex}, \quad (1)$$

where the coefficient a is determined to be 4×10^9 sec^{-1} K^{-2} from the usual formula for thermionic emission. The third term on the right-hand side represents the backflow of excitons with $b = \pi\bar{v}_{ex} \times (3/4\pi n_0)^{2/3}$, where $\bar{v}_{ex}$ is the exciton thermal velocity. For the exciton density n_{ex} outside the condensate we have

$$\dot{n}_{ex} = aNT^2\nu^{2/3}\exp(-\Phi/k_B T) - bN\nu^{2/3}n_{ex} - n_{ex}/\tau_{ex}, \quad (2)$$

where τ_{ex} is the recombination time for free excitons and N is the density of drops. Finally for the free-carrier density $n_{e,h}$ outside the drop we can write

$$\dot{n}_{e,h} = n_{ex}/\tau_{ex} + N\nu/\tau_A - n_{e,h}/\tau_t, \quad (3)$$

where τ_t is the carrier trapping time.

Since both excitons and carriers outside the drops decay rapidly, the lifetime of the signal is governed by the lifetime of the drops. If the system were in thermodynamic equilibrium, the backflow term would be comparable to the evaporation term. However, because of the rapid decay of free excitons the system can be far from

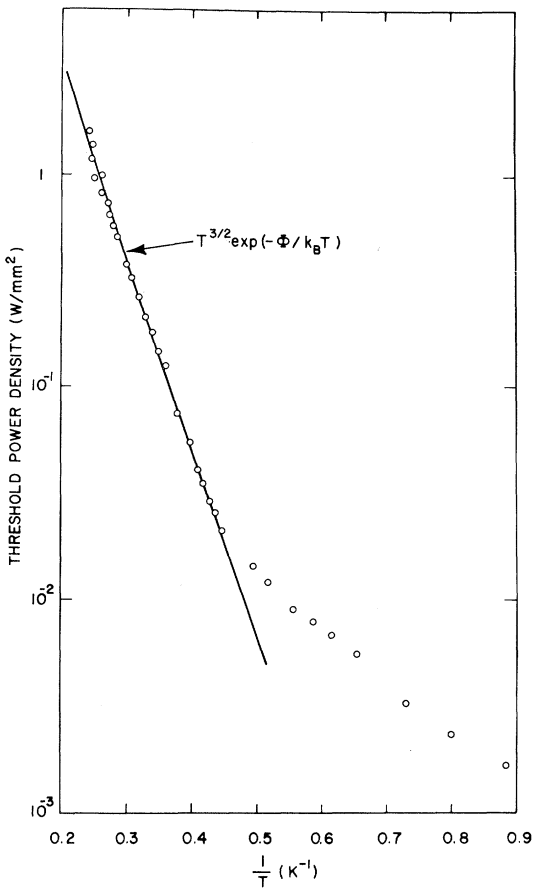

FIG. 2. Optical power threshold for the onset of the long-lived cyclotron resonance signal, detected at a delay time of 10 μsec. The function given in the figure, describing the phase boundary, fits the data above 2 K for a value of $\Phi = 16$ K.

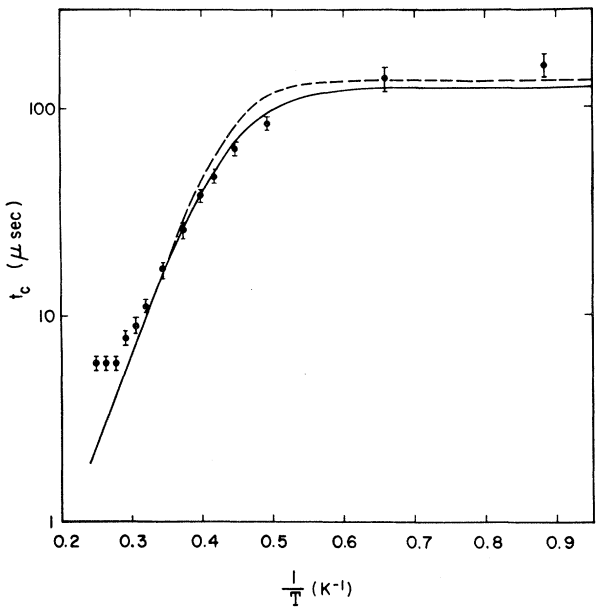

FIG. 3. The cutoff times t_c of the decay profiles of Fig. 1 plotted versus T^{-1}. The data are fitted with curves calculated from the rate equations with $\Phi = 16$ K. The theory with an extra surface emission term (solid curve) fits the data better than without (dashed curve).

equilibrium and we may neglect the backflow. Thus Eq. (1) for ν can be easily solved. The surface terms give a finite cutoff, $\nu(t) = 0$ for $t > t_c$, where t_c is given by

$$t_c = 3\tau_0 \ln[1 + a^{-1}\tau_0^{-1}T^{-2}\nu(0)^{1/3}\exp(\Phi/k_B T)]. \quad (4)$$

When $t_c/3\tau_0 \ll 1$ the logarithm can be expanded and t_c depends exponentially on T^{-1}. In Fig. 3 we have plotted $\ln t_c$ versus T^{-1}. The choice of $\Phi = 16$ K fits the slope of the data for $3.5\ \text{K} > T > 2$ K. From the low-temperature decays (where the thermionic emission term is negligible) we find $\tau_0 = 40 \pm 5$ μsec which predicts 120 μsec for the point at which deviations from the exponential law occur, in agreement with Fig. 3. At temperatures below 1.8 K we choose as the criterion for cutoff $N_e = 5 \times 10^3$ electrons (approximately the noise level; see Fig. 1). The turnover in the data at $T > 3.5$ K presumably signals the increasing importance of backflow which will occur when the exciton density outside becomes large.

The rate equations are integrated straightforwardly to give $n_{e,h}(t)$ with Φ and τ_0 chosen as discussed above. The initial number in a droplet $\nu(0)$ determines the magnitude of $t_c(T)$ and, at our power level of 4×10^{-3} W, we need a value of $\nu(0) = 5 \times 10^8$ which corresponds to a starting radius of 8.4 μm for a droplet. This value is comparable to that determined by light scattering.[3] Finally, we take the decay times τ_A, τ_{ex}, and τ_t as 100, 0.1, and 0.01 μsec, respectively. The results are insensitive to τ_{ex} as long as $\tau_{ex} \lesssim 1$ μsec; τ_t is essentially a scale parameter which was determined by fitting the calculated density of carriers, at $T = 2.5$ K and $t = 10$ μsec, to that observed experimentally. At $T \lesssim 2$ K $n_{e,h}$ is sensitive to τ_A and the choice of $\tau_A = 100$ μsec is in agreement with earlier estimates of the quantum efficiency of the shifted recombination luminescence.[3,4]

In Fig. 1 there is good agreement between experiment and theory above 2 K, but below 2 K we find a somewhat greater deviation from exponential behavior than predicted by the rate equations. We have, therefore, included a surface emission term which is finite at 0 K. This could arise in two ways. One is an elevated e-h temperature relative to the lattice arising from the heat produced by the volume decay processes. Such a temperature correction would change the value of Φ found from the decay curves to 19 K. However, we estimate that an energy of 1 eV per recombination process must be given to the e-h system, which seems unlikely. Alternatively, excitations of the e-h liquid created near the surface by recombination events can have sufficient energy to cause direct exciton emission. Such a temperature-independent term was added to the right-hand side of Eq. (1), corresponding to the direct emission of an exciton for each volume recombination within a surface layer of 0.3 μm. This is approximately the mean free path of an excitation.

We assumed that in the creation process the number of nucleating centers remained fixed and the size of the drops varied with pumping power. Equation (4) then predicts that at fixed temperature, t_c increases with the cube root of the input power. This is experimentally verified, confirming the assumption concerning the nucleation process. From the value $\nu(0)$ used to fit the data and the laser input power we calculate a density of nucleating centers of about 2×10^5 cm^{-3}.

The cyclotron resonance measurements appear to confirm the model of an exciton gas-to-liquid transition and provide a measurement of the internal decay time of the metallic system and also the binding energy. The value found from the cutoff time is 16 K. Observations of the threshold power curve of Fig. 2 lead to an independent value of Φ (16 K). Our values of Φ are substantially lower than those derived from the

position of the shifted luminescence line (30 K, 28 K)[3,4] relative to the peak of the free exciton line. Some of this discrepancy might be attributable to the width of the exciton line, since it seems that the low-energy threshold would be more appropriate than the peak. A value of Φ (17 K) similar to ours was obtained by Pokrovskii[3] from studies of luminescence intensity with power and temperature under steady-state conditions. Theoretical estimates[9,10] give 20 and 29K. Since the discrepancies we are discussing represent only 20% of the correlation energy, the theoretical numbers cannot be relied upon to such accuracy.

In conclusion, observations of the thresholds and decay patterns provide us with information about the energy parameters of the system and insight into the interaction between the droplets and the exciton gas. The good fit obtained to the unusual decay curves confirms the validity of the droplet model.

We thank W. F. Brinkman and E. O. Kane for useful discussions and F. C. Unterwald for technical help in the experiments.

[1]V. M. Asnin and A. A. Rogachev, Zh. Eksp. Teor. Fiz. Pis'ma Red. 7, 464 (1968) [JETP Lett. 7, 360 (1968)].

[2]L. V. Keldysh, in *Proceedings of the Ninth International Conference on the Physics of Semiconductors, Moscow, 1968* (Nauka, Leningrad, 1968), p. 1303.

[3]Ya. E. Pokrovskii, Phys. Status Solidi (a) 11, 385 (1972).

[4]C. Benoît à la Guillaume, M. Voos, and F. Salvan, Phys. Rev. B 5, 3079 (1972).

[5]J. C. Hensel and T. G. Phillips, in Proceedings of the Eleventh International Conference on the Physics of Semiconductors, Warsaw, 1972 (to be published).

[6]V. S. Vavilov, V. A. Zayats, and V. N. Murzin, Pis'ma Zh. Eksp. Teor. Fiz. 10, 304 (1969) [JETP Lett. 10, 192 (1969)].

[7]V. M. Asnin, A. A. Rogachev, and N. I. Sablina, Pis'ma Zh. Eksp. Teor. Fiz. 11, 162 (1970) [JETP Lett. 11, 99 (1970)].

[8]C. Benoît à la Guillaume, M. Voos, F. Salvan, J. M. Laurant, and A. Bonnot, C. R. Acad. Sci., Ser. B 272, 236 (1971).

[9]W. F. Brinkman, T. M. Rice, P. W. Anderson, and S. T. Chui, Phys. Rev. Lett. 28, 961 (1972).

[10]M. Combescot and P. Nozières, J. Phys. C: Proc. Phys. Soc., London 5, 2369 (1972).

Steady-State Motion of Magnetic Domains

A. A. Thiele
Bell Laboratories, Murray Hill, New Jersey 07974
(Received 27 November 1972)

This paper introduces two integrals which simplify calculation of the dynamic properties of magnetic domains. These integrals, over quadratic functions of the spatial derivatives of the magnetization, yield forces acting on a domain which correspond to the gyroscopic and dissipative terms in the Gilbert equation. The force integral corresponging to the gyroscopic term is found to be even less sensitive to the details of the spin distribution than the dissipative drag integral. Hard magnetic bubble domains are considered as an illustrative example.

Recent papers have described the static spin configuration and anomalous dynamic properties of hard magnetic bubbles.[1-6] This paper presents several relations, derived from the Gilbert equation, which greatly facilitate the calculation of some of the dynamic properties of these and other magnetic domains. The relations are applied to the hard-bubble problem as an example. Cartesian tensor notation is used, with repeated indices being assumed summed and with the totally antisymmetric unit tensor being denoted by e_{ijk}. Field position is denoted by x_i and domain position is denoted by X_i. The magnetization is specified either by its three components M_i, or by the saturation magnetization M_s and the polar angles θ and φ. [The z axis (index = 3) corresponds to $\theta = 0$; the x axis (index = 1) corresponds to $\theta = \pi/2$, $\varphi = 0$, the coordinate system being right handed.]

The Gilbert equation, written in tensor notation and arranged in the form which reads, "The time rate of change of angular momentum minus the torque due to linear dissipative effects minus the torque due to reversible effects is equal to zero," is

$$-\frac{1}{|\gamma|}\frac{dM_i}{dt}+\frac{\alpha}{|\gamma|M_s}e_{ijk}M_j\frac{dM_k}{dt} - e_{ijk}M_jH_k{}^r=0, \qquad (1a)$$

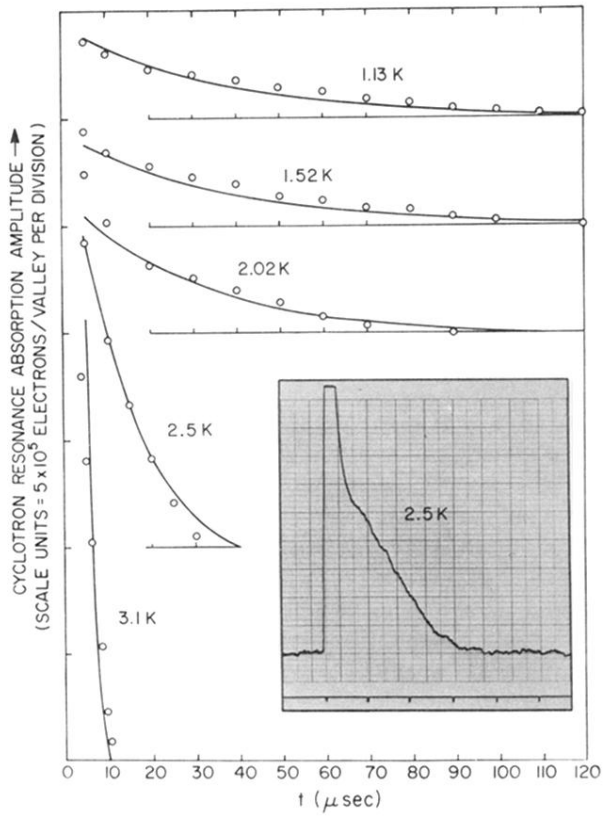

FIG. 1. Decay profiles of the electron cyclotron resonance signal subsequent to Q-switched laser excitation. The inset shows a typical tracing in which a fast signal coincident with the laser pulse is followed by a much slower, nonexponential decay terminated by an abrupt cutoff. In the main figure the solid curves are calculated from the rate equations; the circles represent the data. The data were recorded at a peak optical power level of 4×10^{-3} W (power density, 0.16 W/mm^2).